AD_____

Award Number: W81XWH-07-1-0179

TITLE: Regulation of the mTOR Pathway by a Novel Rheb Binding Protein BNIP3

PRINCIPAL INVESTIGATOR: Kun-Liang Guan, Ph.D.

CONTRACTING ORGANIZATION: University of Michigan
Ann Arbor, MI 48109

REPORT DATE: May 2008

TYPE OF REPORT: Final

PREPARED FOR: U.S. Army Medical Research and Materiel Command
Fort Detrick, Maryland 21702-5012

DISTRIBUTION STATEMENT: Approved for Public Release;
Distribution Unlimited

REPORT DOCUMENTATION PAGE

Form Approved
OMB No. 0704-0188

1. REPORT DATE *(DD-MM-YYYY)*	**2. REPORT TYPE**	**3. DATES COVERED** *(From - To)*
01-05-2008	Final	1 MAY 2007 - 30 APR 2008

4. TITLE AND SUBTITLE

Regulation of the mTOR Pathway by a Novel Rheb Binding Protein BNIP3

5a. CONTRACT NUMBER

5b. GRANT NUMBER
W81XWH-07-1-0179

5c. PROGRAM ELEMENT NUMBER

6. AUTHOR(S)
Kun-Liang Guan, Ph.D.

E-Mail: kuguan@ucsd.edu

5d. PROJECT NUMBER

5e. TASK NUMBER

5f. WORK UNIT NUMBER

7. PERFORMING ORGANIZATION NAME(S) AND ADDRESS(ES)

University of Michigan
Ann Arbor, MI 48109

8. PERFORMING ORGANIZATION REPORT NUMBER

9. SPONSORING / MONITORING AGENCY NAME(S) AND ADDRESS(ES)
U.S. Army Medical Research and Materiel Command
Fort Detrick, Maryland 21702-5012

10. SPONSOR/MONITOR'S ACRONYM(S)

11. SPONSOR/MONITOR'S REPORT NUMBER(S)

12. DISTRIBUTION / AVAILABILITY STATEMENT
Approved for Public Release; Distribution Unlimited

13. SUPPLEMENTARY NOTES

14. ABSTRACT
Uncontrolled mTOR activation is a major contributing factor to the pathogenesis of TSC. mTOR is known to be regulated by a wide range of signals, such hypoxia. The major goal of this project is to determine mTOR regulation by hypoxia. We proposed to focus on BINP3, which is a Rheb interacting protein, in mTOR regulation in response to hypoxia. Our goals outlined in the original proposal have been successfully completed. We confirmed that BNIP3 is indeed a Rheb interaction protein under physiological conditions. We demonstrate that BNIP3 plays a critical role in hypoxia-induced mTOR inhibition. Furthermore, we found that BNIP3 itself has a growth inhibitory activity and inactivation of BNIP3 promotes cell growth in vitro and tumor growth in vivo. Our observation reveals an important mechanism of cell growth regulation by hypoxia. Our results also indicate potential therapeutic target for TSC disease, which has a high level of mTOR and Rheb activation. Activation BNIP3 may inhibit Rheb and mTOR in TSC mutant cells.

15. SUBJECT TERMS
1) TSC; 2) Hypoxia; 3) BNIP3

16. SECURITY CLASSIFICATION OF:			**17. LIMITATION OF ABSTRACT**	**18. NUMBER OF PAGES**	**19a. NAME OF RESPONSIBLE PERSON**
a. REPORT	**b. ABSTRACT**	**c. THIS PAGE**			USAMRMC
U	U	U	UU	19	**19b. TELEPHONE NUMBER** *(include area code)*

Table of Contents

Introduction

The main goal of this idea grant is to demonstrate whether the BNIP3 plays a role in mTOR regulation by Rheb, especially in response to hypoxia stress. BNIP3 is a BH3 domain containing protein in the Bcl2 family. Our preliminary observation indicates that BNIP3 can directly interact with Rheb, which is a direct downstream target of the TSC2 tumor suppressor. TSC2 functions as a GAP to inhibit Rheb, which is a potent activator of mTOR. In TSC mutant cells, mTOR activity is abnormally high. It is widely believed that the uncontrolled mTOR activity contributes to the development of TSC disease. Therefore a key issue TSC research is to understand mTOR regulation. mTOR activity is regulated by a wide range of environmental signals, such as hypoxia. It has been well established that hypoxia inhibits mTOR but the underlining mechanism is not fully understood. Interestingly, hypoxia induces BNIP3. The major hypothesis for this proposal is that BNIP3 may play a critical role in mTOR regulation in response to hypoxia. The main goal of this proposal is to elucidate the molecular mechanism of how hypoxia inhibits cell growth by inhibiting the mTOR pathway and the function of BNIP3 in these processes.

Body

Results summary

Both genetic and biochemical data have established that Rheb is a key upstream activator of mTOR. To search for Rheb interacting proteins, we performed a yeast two-hybrid screen with cDNA libraries from Hela cells and mouse embryos using Rheb as bait. We isolated Bnip3, Bnip3L (Bnip3 like), and PRA1 (prenylated Rab acceptor protein) as positives. Each gene was isolated multiple times as different cDNA clones in our yeast two hybrid screens, indicating true positive interaction of these genes with Rheb in the yeast two-hybrid system. For example, Bnip3 clones were isolated 6 times from the Hela library and 2 times from mouse embryo library. Interestingly, Bnip3 is induced by hypoxia, indicating a potential role of Bnip3 in mTOR regulation in response to hypoxia.

We concentrated our efforts on Bnip3 and Bnip3L because they specifically interacted with Rheb but not other small GTPases. We observed that the interaction between Bnip3 and Rheb in the yeast two-hybrid screen does not depend on the prenylation of Rheb since Bnip3 still showed a positive interaction with Rheb(C181S) mutant. We also observed that Bnip3L interacted with Rheb similarly as Bnip3.

To further confirm the interaction between Bnip3 and Rheb, immunoprecipitation of endogenous proteins was performed. We found endogenous Bnip3 was co-immunoprecipitated (co-IP) with a specific anti-Rheb antibody. In contrast, Bnip3 was not detected in the control immunoprecipitation. It is worth noting that Bnip3 could not be co-immunoprecipitated with Rheb if crosslinking was omitted, indicating that the interaction between Rheb and Bnip3 is transient. These data demonstrate that Bnip3 and Rheb interact under the physiological condition.

Bnip3 contains a central BH3 domain, a conserved domain (CD), and a C-terminal transmembrane domain (TM). Bnip3L (also termed NIX, Nip3-like protein X) is highly homologous to Bnip3 with similar domain structures. However, Bnip3L bears a distinct longer asparagines/proline-rich N terminus. The functions of TM domain and BH3 domain of Bnip3 have been extensively studied. The TM domain of Bnip3 is critical for homodimerization, pro-apoptotic function, and intracellular targeting; whereas deletion of BH3 domain has no effect on the above functions. To examine which domain is involved in interaction with Rheb, we generated a series of deletion mutants as indicated in Fig.1a. The yeast two-hybrid assays

showed none of TM domain, BH3 domain, CD, and N-terminal 30 amino acids are essential for binding, although their binding is less strong than wild type. In contrast, deletion of N-terminal 114 amino acid abolished the binding between Bnip3 and Rheb.

To further confirm the domain in Bnip3 responsible for Rheb binding, HEK293 cells were transiently co-transfected with plasmids expressing various Flag-tagged Bnip3 mutants and Myc-tagged Rheb. Flag-Bnip3 protein was immunoprecipitated by anti-Flag antibody; the associated Myc-Rheb was detected by western blot. Overexpressed Bnip3 has been shown to form a covalently dimer in a TM domain dependent manner. Consistent with published data, the Bnip3-wt, Bnip3ΔN30, Bnip3ΔCD, Bnip3ΔBH3 and Bnip3ΔN114 showed up at twice the size of their predicted monomer molecular weight on the SDS-PAGE gel. In contrast, the Bnip3ΔTM could not form dimers and showed a molecular weight on SDS gel consistent with the predicted monomer. The mutant Rheb(C181S) protein migrated slower on SDS-PAGE gel, which is consistent with earlier studies showing that isoprenylated Rheb migrates more quickly than the unmodified Rheb.

Consistent with two-hybrid results, the CD, BH3 domain and N-terminal 30 amino acids of Bnip3 are not essential for binding with Rheb. Deletion of N-terminal 114 amino acid dramatically decreased the binding. In contrast with the two-hybrid results, however, deletion of TM domain in Bnip3 completely abolished the binding in mammalian cells. Moreover, membrane association is also important for Rheb to interact with Bnip3 because the isoprenylation-defective Rheb(C181S) mutant did not bind with Bnip3 either. The explanation of the difference between the two-hybrid and Co-IP maybe due to the localization of Bnip3 and Rheb are different in these two systems. In the yeast two-hybrid system, Bnip3 and Rheb were fused with LexA activation domain and Gal4 DNA binding domain, respectively. These two fusion proteins are nuclear proteins due to the presence of nuclear localization signals in the fusion proteins. Therefore, the two fusion proteins can interact with each other in the nucleus in the yeast two-hybrid assay. In contrast, deletion of the TM domain in Bnip3 or mutation of the CAAX motif in Rheb will alter their subcellular localizations and prevent the two proteins to see each other in mammalian cells.

To further verify the physical interaction between Bnip3 and Rheb, we constructed YFP–Bnip3 and CFP–Rheb fusion proteins (CFP stands for cyan fluorescent protein and YFP stands for yellow fluorescent protein) and used FRET (Fluorescence Resonance Energy Transfer) measurement techniques to visualize protein interactions in Cos-7 cells. FRET is one of the few tools available to study protein interactions in the cell in real time and also can be an accurate measurement of molecular proximity at angstrom distances (10–100 Å). We found that overexpression of YFP-Bnip3 or CFP-Rheb showed granule-like fluorescence pattern in cytoplasm. In contrast, Bnip3ΔTM and Rheb(C181S) mutant showed homogenous cytoplasmic distribution. These observations demonstrate that the TM domain in Bnip3 and the Cys181 in Rheb are important for subcellular localization of these two proteins. Supporting the Co-IP results in HEK 293 cells, Bnip3 showed strong interaction with Rheb as determined by the FRET. In contrast, no FRET was observed between Bnip3ΔTM and Rheb, nor was observed between Bnip3 and Rheb(C181S). Bnip3ΔN30, Bnip3ΔCD and Bnip3ΔBH3 also displayed a FRET positive interaction with Rheb. As expected, Bnip3 does not interact with Rap1b although the two proteins show similar subcellular distribution. These results further support the interaction between Rheb and Bnip3.

Rheb stimulates S6K phosphorylation and activation via mTOR. Phosphorylation of S6K is a convenient and reliable measurement for mTOR activity in vivo. Therefore, we examined weather Bnip3 modulates the function of Rheb by measuring S6K phosphorylation. In HEK293 cells, overexpression of Flag-Bnip3 inhibited the phosphorylation of the co-transfected HA-S6K1 in a dose dependent manner. Surprisingly, the Bnip3L, which shares more than 50%

sequence identity with Bnip3 and can also bind Rheb, did not have any effect on S6K phosphorylation. These observations strongly suggest that the inhibitory effect of Bnip3 depends on a specific sequence unique in Bnip3 and that mere binding to Rheb is not sufficient to inhibit the ability of Rheb in mTOR activation. 4EBP1 is another target of mTOR. mTOR phosphorylates 4EBP1 at multiple sites, including serine 65. To confirm the inhibitory effect of Bnip3 on mTOR signaling, we examined the effect of Bnip3 on 4EBP1 phosphorylation. Our results showed that Bnip3 but not Bnip3L inhibited 4EBP1 phosphorylation. These observations are consistent with a model that Bnip3 inhibits mTOR activation by Rheb.

Since the Bnip3L has no effect on S6K and 4EBP1 phosphorylation, we focused on Bnip3 in subsequent studies. To further confirm weather Bnip3 inhibits S6K by acting through mTOR, we tested the rapamycin-resistant mutant, S6K-ΔC104, which contains a C-terminal deletion and its phosphorylation of Thr 389 is no longer inhibited by rapamycin. We found Bnip3 could not inhibit phosphorylation of S6K-ΔC104. These results suggest that the inhibitory effect of Bnip3 on S6K likely goes through mTOR. Recently, it has been established the mTOR exists in two functionally distinct complexes, TORC1 and TORC2. TORC1 is responsible for S6K Thr389 phosphorylation while TORC2 phosphorylates AKT S473. To check weather Bnip3 inhibits TORC2 activity, we examined the effect of Bnip3 overexpression on phosphorylation of GST-Akt. Our results demonstrate that Bnip3 is unable to inhibit the phosphorylation of Akt. This data implies that Bnip3 specifically inhibits TOCR1 functions, but not TOCR2. Our data are consistent with the notion that Rheb is not directly involved in TORC2 activation.

To map the sequence in Bnip3 required for S6K inhibition, several Bnip3 mutants were co-transfected with HA-S6K. Bnip3 wild type could potently inhibit S6K phosphorylation. Deletion of BH3 domain and CD had no effect on the ability of Bnip3 to inhibit S6K. As anticipated, Bnip3ΔTM completely lost its ability to inhibit S6K because this mutant could not bind Rheb. Bnip3ΔN30, which could bind Rheb at a similar level as the wild type Bnip3, however also lost its activity completely. As predicted, Bnip3-ΔN114 could not inhibit S6K phosphorylation. These results suggest that interaction between Bnip3 and Rheb is necessary but not sufficient to inhibit Rheb function. Furthermore, our data indicates that the N-terminal region of Bnip3 is required to inhibit the mTOR pathway. Interestingly, the N-terminal region is not conserved between Bnip3 and Bnip3L, consistent with the observation that Bnip3L cannot inhibit mTOR although it binds Rheb. Given the fact that Bnip3 and Bnip3L has no homolog in N-terminal 30 amino acids but shares 65% identity in the rest of the protein, the above results strongly suggested the N-terminal 30 amino acids of Bnip3 are essential for S6K inhibition.

To examine weather Bnip3 affect the Rheb-induced S6K phosphorylation, Bnip3 was co-transfected with Myc-Rheb into HEK 293 cells. Cells were treated with D-PBS to reduce the basal S6K phosphorylation, therefore, the D-PBS treatment highlighted the stimulatory effect of Rheb on S6K. Overexpression of Flag-Bnip3 compromised the S6K phosphorylation induced by Rheb co-expression. We also examined the phosphorylation of 4EBP1, another substrate of TORC1. Flag-Bnip3 inhibited the Rheb-induced 4EBP1 phosphorylation. The data in figure 2 indicate that mere binding is not sufficient for Bnip3 to inhibit Rheb function.

To investigate how Bnip3 affects Rheb function, we tested Rheb GTP/GDP radio by overexpressing Bnip3 and Rheb in HEK 293 cell. Overexpression of wild type Bnip3 reproducibly decreased the GTP/GDP radio by approximately 30% (Fig.3c). Although, the effect of Bnip3 on Rheb GTP/GDP radio is moderate, this change in Rheb GTP/GDP is rather significant. In similar experiments, we could not detect a change in Rheb GTP/GDP under various conditions, including insulin stimulation and amino acid addition. Further supporting the importance of Bnip3 on Rheb GTP levels, we tested Bnip3ΔTM and Bnip3ΔN30, which lost the ability to inhibit S6K phosphorylation. We found that neither Bnip3ΔTM nor Bnip3ΔN30

affected Rheb GTP levels. Besides TSC2, Bnip3 is the only protein known to affecting Rheb GTP/GDP in our studies. Therefore, our data indicate that Bnip3 inhibits the mTOR pathway by decreasing Rheb GTP levels.

We used siRNA (small interference RNA) oligonucleotides to test the effect of endogenous Bnip3 on S6K phosphorylation and S6K kinase activity, which was measured by checking the phosphorylation of S6, a directly substrate of S6K. Two RNA duplexes, corresponding to either an amino-terminal (Bnip3-N) or C-terminal (Bnip3-C) region of Bnip3, were used to suppress expression of endogenous Bnip3. Transfection of siRNA-C or siRNA-N caused a significant reduction of endogenous Bnip3 protein levels in HEK293 cells, whereas Bnip3 siRNA had no effect on expression levels of the β-actin control. It is worth noting that in contrast to a strong induction of Bnip3 by hypoxia in many cell lines, Bnip3 is expressed in HEK 293 cells and its expression is not significantly induced by one hour exposure to hypoxia. We found that Bnip3 knockdown had little effect on the basal phosphorylation of S6K and S6. Hypoxia inhibited S6K phosphorylation. Interestingly, Bnip3 knockdown significantly blocked the inhibition of S6K phosphorylation in response to hypoxia. Control experiments with unrelated siRNA oligonucleotides had no effect on the phosphorylation of S6K and S6. This observation suggests that Bnip3 may be specifically activated under hypoxia and plays a critical role in mTOR inhibition in response to hypoxia.

To further confirm the specific function of Bnip3 in hypoxia response, we established Bnip3 knockdown stable cell line. HEK293 cells were infected by retrovirus expressing Bnip3 shRNA (small hairpin RNA) and control shRNA respectively. The stable shRNA expressing cells were selected by puromycin. Bnip3 protein was greatly reduced in the Bnip3-shRNA expressing cells lines. Consistent with the transient siRNA transfection results, stable Bnip3 knockdown blocked the decrease of phosphorylation of S6K and S6, in response to hypoxia conditions, but had no effect on phosphorylation of Akt. We also examined if the effect of Bnip3 is specific to hypoxia response. Both hypoxia and low pH (pH 6.5) caused a similar reduction in phosphorylation of S6K and S6. Bnip3 knockdown only suppressed the effect of hypoxia but not the effect of low pH. These results suggest that Bnip3 is specifically involved in hypoxia response. In addition, cells were treated with a low dose of Rapamycin to partially inhibit TORC1 activity to a degree similar to those inhibited by either hypoxia or low pH. Bnip3 siRNA could not block the inhibitory effect of Rapamycin on S6K. These data suggest that Bnip3 acts specifically in hypoxia response upstream of TORC1. Moreover, the above results are consistent with our observations that Bnip3 binds to Rheb and decreases Rheb GTP levels.

Bnip3 has been implicated in tumor development. A possible mechanism of Bnip3 in cancer inhibition is due to its activity in promoting cell death. It is also possible that Bnip3 may inhibit tumor growth by inhibiting mTOR, especially in solid tumors, which are frequently under hypoxia conditions. We tested the effect of Bnip3 knockdown on tumor formation in nude mice. Both Bnip3 knockdown and control HEK293 cells were injected into nude mice. Tumor size was monitored. We found that the Bnip3 knockdown cells formed much bigger tumor than the control cells. These data indicate that the elevated mTOR activity in the Bnip3 knockdown cells may provide a growth advantage. To further test the function of mTOR activation in Bnip3-induced tumor growth, we treated the mice with rapamycin, which should inhibit mTOR even in Bnip3 knockdown cells. As expected, rapamycin significantly inhibited tumor growth of HEK293 cells. Interestingly, the Bnip3 knockdown cells did not show any growth advantage over the control cells in the presence of rapamycin. These results strongly indicate that the elevated mTOR activity by Bnip3 knockdown is responsible for the growth advantage of the Bnip3 knockdown in HEK293 cells in vivo.

Key Research Accomplishments

1. We identified Bnip3 as a Rheb specific interacting protein.
2. We demonstrated that Bnip3 inhibits the ability of Rheb in mTOR activation.
3. We found that Bnip3 decreases Rheb-GTP, therefore inhibiting Rheb.
4. We showed that Bnip3 mediates the hypoxia response in mTOR inhibition.
5. We found that Bnip3 inhibits cell growth in response to hypoxia.
6. We presented evidence to support Bnip3 as a tumor suppressor by inhibiting cell growth.

Reportable Outcomes

Li, Y., Wang, Y., Kim, E., Beemiler, P., Wang, C-Y., Swanson, J., You, M., and Guan, K-L. (2007) Bnip3 mediates the hypoxia-induced inhibition on mTOR by interacting with Rheb. J. Biol. Chem. 282, 35803-13.

Conclusions

Our studies demonstrate that Bnip3, a hypoxia inducible BH3 domain containing protein, directly binds Rheb and inhibits the mTOR pathway. Bnip3 decreases Rheb GTP levels in a manner depending on the binding to Rheb and the presence of the N-terminal domain. Both knockdown and overexpression experiments show that Bnip3 plays an important role in mTOR inactivation in response to hypoxia. Moreover, Bnip3 inhibits cell growth in vivo by suppressing the mTOR pathway. These observations demonstrate that Bnip3 mediates the inhibition of mTOR pathway in response to hypoxia. These data provide a biochemical mechanism that Bnip3 functions as a tumor suppressor by inhibiting cell growth in response to hypoxia.

References

Appendices

See the attached paper.

THE JOURNAL OF BIOLOGICAL CHEMISTRY VOL. 282, NO. 49, pp. 35803–35813, December 7, 2007

Bnip3 Mediates the Hypoxia-induced Inhibition on Mammalian Target of Rapamycin by Interacting with Rheb*

Received for publication, June 26, 2007, and in revised form, September 12, 2007 Published, JBC Papers in Press, October 10, 2007, DOI 10.1074/jbc.M705231200

Yong Li[‡], Yian Wang[§], Eunjung Kim[‡], Peter Beemiller[¶], Cun-Yu Wang[‖], Joel Swanson[¶], Ming You[§], and Kun-Liang Guan[‡‡‡1]**

*From the [‡]Life Sciences Institute, the **Department of Biological Chemistry, the [‡‡]Institute of Gerontology, the [¶]Department of Microbiology and Immunology, and the [‖]Department of Biologic and Materials Sciences, University of Michigan, Ann Arbor, Michigan 48109 and the [§]Department of Surgery and Alvin J. Siteman Cancer Center, Washington University School of Medicine, St. Louis, Missouri 63110*

The mammalian target of rapamycin (mTOR) is a central controller of cell growth, and it regulates translation, cell size, cell viability, and cell morphology. mTOR integrates a wide range of extracellular and intracellular signals, including growth factors, nutrients, energy levels, and stress conditions. Rheb, a Ras-related small GTPase, is a key upstream activator of mTOR. In this study, we found that Bnip3, a hypoxia-inducible Bcl-2 homology 3 domain-containing protein, directly binds Rheb and inhibits the mTOR pathway. Bnip3 decreases Rheb GTP levels in a manner depending on the binding to Rheb and the presence of the N-terminal domain. Both knockdown and overexpression experiments show that Bnip3 plays an important role in mTOR inactivation in response to hypoxia. Moreover, Bnip3 inhibits cell growth *in vivo* by suppressing the mTOR pathway. These observations demonstrate that Bnip3 mediates the inhibition of the mTOR pathway in response to hypoxia.

Target of rapamycin (TOR),[2] is an evolutionarily conserved serine/threonine kinase that plays a central role in cell growth (1–3). TOR regulates many processes, including protein translation, ribosome biogenesis, autophagy, and metabolism. TOR functions to integrate a wide range of extracellular and intracellular signals to produce a concerted cellular response, such as to stimulate cell growth. For example, mammalian target of rapamycin (mTOR) is activated by growth factor and nutrient availability. In contrast, mTOR is inhibited by cellular energy starvation and various stress conditions, including osmotic stress and hypoxia. These observations established a fundamental importance of mTOR in signal integration in regulation of cell growth.

Recent studies have demonstrated that TOR exists in two functionally distinct protein complexes, termed TOR complex 1 (TORC1) and TOR complex 2 (TORC2) (3, 4). The two TOR complexes were initially identified in yeast and subsequently were also characterized in *Drosophila* and mammalian cells. TORC1 contains mTOR, mLST8, PRAS40, and Raptor, whereas TORC2 contains mTOR, mLST8, Rictor, and Sin1 (5–12). TORC1 is responsible for phosphorylation of Thr^{389} of S6K1 (ribosomal protein S6 kinase) and 4EBP1 (eukaryote initiation factor 4E-binding protein), two important regulators in protein synthesis (1). In contrast, TORC2 has different substrates and is responsible for phosphorylation of the hydrophobic sites in both AKT and PKC (9, 13). Interestingly, TORC1 but not TORC2 is inhibited by rapamycin (6, 8, 9). These observations clearly demonstrate that the two TOR complexes have different physiological functions *in vivo*.

Much progress has been made regarding the mechanisms of TORC1 regulation. Tuberous sclerosis complex (TSC) is a genetic disease characterized by benign hamartomas in various tissues (14). Mutations in either the TSC1 or TSC2 tumor suppressor gene are responsible for TSC development. TORC1 is highly activated in TSC tumors or cells with mutation of either TSC1 or TSC2. Both genetic and biochemical data have demonstrated that TSC1 and TSC2 are upstream negative regulators of TORC1. TSC2 has GTPase-activating protein activity specifically toward Rheb (Ras homolog enriched in brain), and Rheb is a potent upstream activator of TORC1 (15–21). Interestingly, Rheb may activate TORC1 by direct binding (11, 22, 23). Therefore, a signaling pathway from TSC1-TSC2 to Rheb to TORC1 has been established.

TORC1 is regulated by a wide range of intracellular and extracellular signals, and the TSC1-TSC2 complex appears to play an important role in receiving and integrating multiple signals to control TORC1 activity (3, 4). It has been shown that TSC2 is phosphorylated and possibly inactivated by AKT, which is a key downstream signaling molecule in growth and insulin signaling (24–27). TSC2 phosphorylation has also been reported to play a critical role in cellular energy response. Energy starvation activates AMPK that inhibits the mTOR pathway by phosphorylating TSC2 (28, 29).

Rheb is a Ras family small GTPase, conserved from yeast to mammals (30). Rheb specifically activates TORC1 and enhances S6K phosphorylation in a rapamycin-sensitive manner (31) but does not activate TORC2 (31, 32). Like other Ras

* This work is supported by grants from National Institutes of Health and the Department of Defense (to K. L. G.). The costs of publication of this article were defrayed in part by the payment of page charges. This article must therefore be hereby marked "*advertisement*" in accordance with 18 U.S.C. Section 1734 solely to indicate this fact.

[1] To whom correspondence should be addressed: Dept. of Pharmacology and Moores Cancer Center, University of California at San Diego, La Jolla, CA 92093. E-mail: kunliang@umich.edu.

[2] The abbreviations used are: TOR, target of rapamycin; mTOR, mammalian target of rapamycin; TORC1 and TORC2, TOR complex 1 and 2, respectively; TSC, tuberous sclerosis complex; TM, transmembrane; BH3, Bcl-2 homology 3; CD, highly conserved domain; IP, immunoprecipitation; FRET, fluorescence resonance energy transfer; siRNA, small interfering RNA; RNAi, RNA interference; YFP, yellow fluorescent protein; CFP, cyan fluorescent protein; HA, hemagglutinin.

family GTPases, the GTP-bound Rheb is active, whereas the GDP-bound Rheb is inactive to stimulate S6K phosphorylation (33). However, besides the TSC2 GTPase-activating protein, which inhibits Rheb by stimulating GTP hydrolysis, how Rheb activity is regulated is rather unclear. For example, conflicting results have been reported concerning whether amino acids, which potently stimulate TORC1 activity, increase Rheb GTP levels (34–36).

Among many stress conditions that inhibit TORC1, the hypoxia-induced TORC1 inactivation may play an important role in tumor growth. Two hypoxia-inducible genes, Redd1 and Redd2 (also known as RTP80 and RTP80L) have been implicated to mediate the TORC1 inactivation in response to hypoxia (37–39). However, the biochemical mechanism of how Redd1/Redd2 inhibit TORC1 is unclear, but they may act upstream of TSC2.

Bnip3 (Bcl-2/adenovirus E1B 19-kDa interacting protein 3) is a hypoxia-induced pro-death protein that belongs to the Bcl-2 superfamily (40, 41). Bnip3 contains a C-terminal transmembrane (TM) domain, a sequence resembling the Bcl-2 homology 3 (BH3) domain and a highly conserved domain (CD) (Fig. 1*a*) (42). Bnip3 was reported to have proapoptotic function (43). Recent studies have highlighted the unique characteristics of Bnip3 in inducing cell death and hypoxia response. The pro-death function of Bnip3 requires the transmembrane domain but not the BH3 domain, indicating that Bnip3 promotes cell death different from the conventional BH3-only proteins that normally neutralize prosurvival Bcl-2 family protein by interacting via their BH3 domain. Consistent with this observation, Bnip3-induced cell death is caspase-independent (44, 45). Currently, the mechanism of induction of cell death by Bnip3 is unclear, but autophagic death and necrosis-like cell death have been suggested (45, 46).

Bnip3 is strongly induced by hypoxia and plays a role in hypoxic cell death in cancer cells and cardiomyocytes (47–49). Transcriptional silencing of Bnip3 has been reported in gastrointestinal cancers, and probably contributes to resistance to hypoxia-induced cell death in those cancers (50–52). In addition, knockdown Bnip3 enables breast cancer metastases in the lung, liver, and bone (53).

In this study, we identified Bnip3 as a Rheb-binding protein. Our results show that Bnip3 inhibits the ability of Rheb to activate TORC1 and mediates the inhibitory effect of hypoxia on mTOR signaling. These data provide a biochemical mechanism that Bnip3 functions as a tumor suppressor by inhibiting cell growth in response to hypoxia.

MATERIALS AND METHODS

Antibodies and Plasmids—Anti-phospho-S6K(Thr^{389}), Anti-phospho-S6(Ser$^{230/244}$), and anti-phospho-AKT(Ser^{473}) were purchased from Cell Signaling Inc. Anti-Myc and anti-HA antibodies were purchased from Covance. Anti-FLAG was purchased from Cayman. Anti-Bnip3 (clone ANA30) was purchased from Sigma. Anti-actin was from Santa Cruz Biotechnology, Inc. (Santa Cruz, CA). Anti-Rheb antibody was made by immunized rabbit with GST-Rheb protein (Pocono Rabbit Farm and Laboratory).

PcDNA-HA-S6k, PcDNA-HA-S6kΔC104, GST-Akt, and pRK5-myc-Rheb constructs were described previously (27). All point mutation constructs of Rheb were generated by the QuikChange site-directed mutagenesis kit (Stratagene) and verified by DNA sequencing. All deletion constructs of Bnip3 were generated by a standard PCR cloning strategy, using the pcDNA3-FLAG-Bnip3 construct as a template.

Yeast Two-hybrid Assays—The *Saccharomyces cerevisiae* strain L40 was co-transformed with bait plasmids expressing Rheb fusions to the LexA-DNA binding domain in pLexAde and with a HeLa cell cDNA library constructed in pGAD-GH (laboratory stock). About 5×10^6 clones were screened for *HIS3* and *lacZ* gene expression using protocols as described (54). Positive clones were verified by reassessing for growth on $Trp^-/Leu^-/His^-$ plates and galactosidase activity by co-transforming bait plasmid and pGAD-GH vectors derived from positive yeast clones. For transformants that remained positive with the bait but negative with the vector alone, plasmid DNA was isolated, transformed into *E. coli* DH10B, and subjected to further detailed analyses, including sequencing and co-immunoprecipitation.

Cell Culture—HEK293 cells were routinely cultured in Dulbecco's modified Eagle's medium containing 10% fetal bovine serum in a 37 °C incubator with 5.0% CO_2. For hypoxia conditions, cells were maintained at 37 °C within a modular incubator chamber (BioSpherix) filled with 5.0% CO_2 and 0.1% O_2 (balanced with N_2). The concentration of oxygen in the hypoxia chamber was continuously monitored and maintained at 0.1% O_2 (0.75 mm Hg) by a gas oxygen controller (PROOX model 110; BioSpherix). All of the hypoxia treatments were performed in the above condition for 1 h.

Transfection and Western Blot Analysis—Transfection was performed in serum-free conditions using Lipofectamine™ reagent (Invitrogen) following the manufacturer's instructions. Cells were lysed in Lysis Buffer A (10 mM Tris-HCl, pH 7.5, 100 mM NaCl, 1% Triton X-100, 50 mM NaF, 2 mM EDTA, 1 mM phenylmethylsulfonyl fluoride, 10 μg ml^{-1} leupeptin, 10 μg ml^{-1} aprotinin). Samples were resolved by 12.5% SDS-PAGE, and proteins were transferred to polyvinylidene difluoride and then blotted with the desired antibodies.

Immunoprecipitation—The co-immunoprecipitations (co-IPs) of Bnip3 and Rheb were performed as following procedure similar to that described by Kim *et al.* (68). Briefly, 1 g of liver tissue from a C57BL/6J mouse was homogenized in 5 ml of ice-cold Lysis Buffer B (2.5 mg/ml dithiobis(succinimidyl propionate), 30 mM HEPES (pH 7.5), 120 mM NaCl, 1 mM EDTA, 10 mM pyrophosphate, 1% Triton X-100, and one tablet of protease inhibitors (Roche Applied Science)). Cross-linking reactions were performed with dithiobis(succinimidyl propionate) and stopped by adding 500 μl of 1 M Tris-HCl (pH 7.4) followed by an additional 15-min incubation. The samples were briefly centrifuged to remove any insoluble debris. The supernatant was split to two equal aliquots. Anti-Rheb antibody and control IgG antibody were added separately to these two aliquots for immunoprecipitation. Antibody was incubated for 2 h at 4 °C. Then 20 μl of a 50% slurry of protein G-Sepharose was added and rotated for 1 h. Immunoprecipitates were collected by centrifugation and washed three times with Lysis Buffer A with 500

mM NaCl and 0.05% SDS. Immunocomplexes were subjected to SDS-PAGE and Western blotting.

Fluorescence Resonance Energy Transfer (FRET) Microscopy—FRET imaging was performed on an inverted Nikon Eclipse TE300 microscope (Nikon USA, Melville, NY) with a ×60, 1.4 numerical aperture, oil immersion PlanApo objective lens and a Lambda LS xenon arc lamp with liquid light guide (Sutter Instrument, Novato, CA) for epifluorescent illumination. Wavelength selection for excitation and emission was controlled by a Lambda 10-2 filter wheel (Sutter Instruments) and JP4v2 filter set (Chroma Technology, Rockingham, VT) to record the component fluorescence images I_D (excitation at 430 ± 12.5 nm, emission at 470 ± 15 nm), I_A (excitation at 500 ± 10 nm, emission at 535 ± 15 nm), and I_F (excitation at 430 ± 12.5 nm, emission at 535 ± 15 nm). Fluorescence images were recorded with a CoolSnap HQ cooled CCD camera (Roper Scientific, Tucson, AZ). Image acquisition and processing was performed in Metamorph 6.2 (Universal Imaging, Melville, PA). Bias images were acquired with the microscope illumination path blocked. Images were shade- and bias-corrected before further image arithmetic.

Calculation of the FRET stoichiometry images E_A, E_D, E_{AVG}, and R_M from the component fluorescence images was performed as described previously (69, 71). The processed images represent the fraction of donor in donor-acceptor complexes (f_d) multiplied by E_C (E_D), the fraction of acceptor in donor-acceptor complexes (f_A) multiplied by E_C (E_A), and the ratio of total acceptor to total donor (R_M) (71). E_C represents the characteristic energy transfer efficiency of BIP3-CFP-Rheb-YFP complexes. However, the numerical value of E_C is not required to calculate the FRET stoichiometry images E_A, E_D, and R_M. E_{AVG} is the arithmetic mean of E_A and E_D and adjusts for differences in acceptor-donor ratios observed in different cells (69).

Measurement of GDP/GTP Ratio of Rheb—The experiment was done as previously described (33). HEK293 cells were transfected with the indicated Rheb and/or Bnip3 expression plasmids. Thirty-six hours after transfection, the cells were incubated with phosphate-free Dulbecco's modified Eagle's medium containing 25 μCi of [^{32}P]phosphate for 4 h. After the labeling, cells were lysed with 200 μl of lysis buffer (0.5% NP-30, 50 mM Tris (pH 7.5), 100 mM NaCl, 10 mM $MgCl_2$, 1 mM dithiothreitol, 1 mM phenylmethylsulfonyl fluoride, 10 μg/ml leupeptin, 10 μg/ml aprotinin) per well of 6-well plates. The Myc-Rheb was immunoprecipitated by anti-Myc antibody. The Rheb-bound nucleotides were eluted with 20 μl of elution buffer (2 mM EDTA, 0.2% SDS, 1 mM GDP, 1 mM GTP) at 68 °C for 10 min. GTP and GDP were resolved by thin layer chromatography and visualized by a PhosphorImager.

Transit Knockdown of Bnip3 in HEK293 Cells—Short interfering RNA (siRNA) oligonucleotides against Bnip3 were purchased from Dharmacon. siRNA-N and siRNAi-C represent double-stranded RNA oligonucleotides corresponding to N-terminal and C-terminal sequence of Bnip3. The negative control siRNA oligonucleotides were purchased from Invitrogen. HEK293 cells were transfected with 200 ng of RNAi using Lipofectamine reagent, as described above. The level of endogenous Bnip3 was determined by immunoblotting with an anti-Bnip3 antibody. The sequences of siRNA oligonucleotides were as follows: Bnip3 siRNA-N, 5′-ucgcagacaccacaagaua; Bnip3 siRNA-C, 5′-gaucauauuggaaggcgu; control siRNA, 5′-ccaugggacuaacuagu.

Generation of Stable Small Hairpin RNA (shRNA)-expressing HEK293 Cell Line—The Bnip3 siRNA-expressing cells were established by pSuper siRNA delivery system (OligoEngine, Inc.) following the manufacturer's protocol. Briefly, two pairs of oligonucleotides were synthesized by Invitrogen to construct Bnip3 siRNA expression vector (pSuper.puro-Bnip3.RNAi) and control siRNA expression vector (pSuper.puro-con.RNAi). Oligonucleotides were annealed and ligated into BamHI- and BglII-cut pSuper-puro vectors. The sequences of Bnip3 shRNA and control shRNA coding sequences were as follows: Bnip3 forward, 5′-gatcccctcgcagacaccacaagatattcaagagatatcttgtggtgtctgcgattttta; Bnip3 reverse, 5′-agcttaaaaatcgcagacaccacaagatatctcttgaatatcttgtggtgtctgcgaggg; control forward, 5′- gatcccccatgggactaactagtttcaagagaactagttagtcccatggttttta; control reverse, 5′-agcttaaaaaccatgggactaactagttctcttgaaactagttagtcccatggggg.

pSuper.puro-Bnip3.RNAi and pSuper.puro-con.RNAi were transfected into Phoenix cells with Lipofectamine. The virus-containing culture medium was collected at 48 h after transfection. HEK293 cells were infected by retrovirus expressing Bnip3 shRNA and control shRNA separately. After 48 h of infection, the shRNA-expressing cells were selected with 2 μg/ml of puromycin.

Nude Mouse Tumorigenesis Assay with siRNA-BNIP3—The HEK293 cells were cultured in Dulbecco's modified Eagle's medium supplemented with 10% fetal bovine serum and 2 μg/ml puromycin at 37 °C and in a 5% CO_2 atmosphere. The tumorigenicity of HEK293 cells was assayed by subcutaneous injection of equal cells (1.5 or 3 million) suspended in 200 μl of serum-free Dulbecco's modified Eagle's medium into the back of ~7-week-old male athymic mice (Hsd:Athymic Nude-*nu* (*nu*/*nu*), which were obtained from Harlan (Indianapolis, IN). The mice were housed in the institutional animal facilities. Food and water were given *ad libitum*. All animal works were performed under protocols approved by the Washington University School of Medicine Institutional Animal Care and Use Committee. Puromycin was obtained from Sigma (P7255; Sigma). After HEK293 cell injection, tumor size was measured with calipers in three dimensions at times as indicated. Tumor volume was calculated using the formula for volume of an ellipsoid: $4/3 \times L/2 \times W/2 \times H/2$, where L represents length, W is width, and H is height (70). All mice were sacrificed by asphyxiation with CO_2 on day 20, tumors were removed, and tumor weight (g) was measured. A two-tailed t test was used.

RESULTS

Identification of Bnip3 as a Rheb-binding Protein—Both genetic and biochemical data have established that Rheb is a key upstream activator of mTOR. Although Rheb has been shown to interact with mTOR, the interaction between Rheb and mTOR does not depend on the GTP binding status of Rheb, raising the question regarding the functional significance of this interaction (23). To search for Rheb-interacting proteins, we performed a yeast two-hybrid screen with cDNA libraries from HeLa cells and mouse embryos using Rheb as bait. We isolated

TABLE 1
Interaction between Rheb and Bnip3 in the yeast two-hybrid assay

DNA-binding domain construct pLexA	DNA activation domain construct pGAD	Growth on $Leu^-/Trp^-/His^-$ medium	β-Galactosidase staining
Rap1b	Bnip3 wild type	−	−
	PRA1	+	++++
Rheb	Bnip3 wild type	+	+++
	Bnip3ΔN30	+	++
	Bnip3ΔN114	−	−
	Bnip3ΔBH3	+	++
	Bnip3ΔTM	+	++
	Bnip3ΔCD	+	++
	PRA1	+	++++
Rheb(C181S)	Bnip3 wild type	+	++
	PRA1	−	−

Bnip3, Bnip3L (Bnip3-like), and PRA1 (prenylated Rab acceptor protein) as positives. Each gene was isolated multiple times as different cDNA clones in our yeast two-hybrid screens, indicating true positive interaction of these genes with Rheb in the yeast two-hybrid system. For example, Bnip3 clones were isolated six times from the HeLa library and two times from mouse embryo library. PRA1 has been shown to interact with several small GTPases (including Ras, Rap, Rho, TC21, and Rab) in a prenylation-dependent manner (54). Rheb protein is isoprenylated at the C-terminal CAA*X* motif. To examine whether isoprenylation of Rheb is required for interaction with PRA1, we tested the isoprenylation-defective Rheb(C181S) mutant, in which the cysteine within the CAA*X* motif was substituted by a serine. As predicted, PRA1 could not interact with the Rheb(C181S) mutant (Table 1). This observation suggests that PRA1 interacts with Rheb requires the C-terminal isoprenylation. PRA1 has been suggested to act as an escort protein for small GTPases by binding to the hydrophobic isoprenoid moieties of the small GTPases and facilitates their trafficking through the endomembrane system (54). Therefore, PRA1 may have a similar function for Rheb intracellular trafficking.

We concentrated our efforts on Bnip3 and Bnip3L, because they specifically interacted with Rheb but not other small GTPases. For example, Bnip3 did not interact with Rap1b (Table 1), which is the closest homolog of Rheb. We observed that the interaction between Bnip3 and Rheb in the yeast two-hybrid screen does not depend on the prenylation of Rheb, since Bnip3 still showed a positive interaction with Rheb(C181S) mutant (Table 1). We also observed that Bnip3L interacted with Rheb similarly as Bnip3 (data not shown).

To further confirm the interaction between Bnip3 and Rheb, immunoprecipitation of endogenous proteins was performed. We found that endogenous Bnip3 was co-immunoprecipitated with a specific anti-Rheb antibody (Fig. 1*b*). In contrast, Bnip3 was not detected in the control immunoprecipitation. It is worth noting that Bnip3 could not be co-immunoprecipitated with Rheb if cross-linking was omitted, indicating that the interaction between Rheb and Bnip3 is transient. These data demonstrate that Bnip3 and Rheb interact under physiological conditions.

Binding of Bnip3 and Rheb Dependent on Membrane Localization of both Proteins—Bnip3 contains a central BH3 domain, a CD, and a C-terminal TM domain (Fig. 1*a*). Bnip3L (also termed NIX (Nip3-like protein X)) is highly homologous to Bnip3 with similar domain structures (55). However, Bnip3L bears a distinctly longer asparagine/proline-rich N terminus (56). The functions of the TM domain and BH3 domain of Bnip3 have been extensively studied (44, 57). The TM domain of Bnip3 is critical for homodimerization, proapoptotic function, and intracellular targeting, whereas deletion of the BH3 domain has no effect on the above functions. To examine which domain is involved in interaction with Rheb, we generated a series of deletion mutants as indicated in Fig. 1*a*. The yeast two-hybrid assays showed that none of TM domain, BH3 domain, CD, and N-terminal 30 amino acids are essential for binding, although their binding is less strong than wild type (Table 1). In contrast, deletion of the N-terminal 114 amino acids abolished the binding between Bnip3 and Rheb.

To further confirm the domain in Bnip3 responsible for Rheb binding, HEK293 cells were transiently co-transfected with plasmids expressing various FLAG-tagged Bnip3 mutants and Myc-tagged Rheb. FLAG-Bnip3 protein was immunoprecipitated by anti-FLAG antibody; the associated Myc-Rheb was detected by Western blot (Fig. 1*c*). Overexpressed Bnip3 has been shown to form a covalent dimer in a TM domain-dependent manner (58). Consistent with published data, the Bnip3-wt, Bnip3ΔN30, Bnip3ΔCD, Bnip3ΔBH3, and Bnip3ΔN114 showed up at twice the size of their predicted monomer molecular weights on the SDS-PAGE gel (Fig. 1*c*). In contrast, the Bnip3ΔTM could not form dimers and showed a molecular weight on SDS gel consistent with the predicted monomer (58, 59). The mutant Rheb(C181S) protein migrated slower upon SDS-PAGE, which is consistent with earlier studies showing that isoprenylated Rheb migrates more quickly than the unmodified Rheb (60).

Consistent with two-hybrid results, the CD, BH3 domain, and N-terminal 30 amino acids of Bnip3 are not essential for binding with Rheb. Deletion of the N-terminal 114 amino acids dramatically decreased the binding. In contrast with the two-hybrid results, however, deletion of the TM domain in Bnip3 completely abolished the binding in mammalian cells (Fig. 1*c*). Moreover, membrane association is also important for Rheb to interact with Bnip3, because the isoprenylation-defective Rheb(C181S) mutant did not bind with Bnip3 either (Fig. 1*c*). The explanation of the difference between the two-hybrid and co-IP results may be due to the fact that the localizations of Bnip3 and Rheb are different in these two systems. In the yeast two-hybrid system, Bnip3 and Rheb were fused with the LexA activation domain and Gal4 DNA binding domain, respectively. These two fusion proteins are nuclear proteins due to the presence of nuclear localization signals in the fusion proteins. Therefore, the two fusion proteins can interact with each other in the nucleus in the yeast two-hybrid assay. In contrast, deletion of the TM domain in Bnip3 or mutation of the CAA*X* motif in Rheb will alter their subcellular localizations and prevent the two proteins from seeing each other in mammalian cells.

To further verify the physical interaction between Bnip3 and Rheb, we constructed YFP-Bnip3 and CFP-Rheb fusion proteins and used FRET measurement techniques to visualize protein interactions in COS-7 cells. FRET is one of the few tools available to study protein interactions in the cell in real time and also can be an accurate measurement of molecular proximity at angstrom distances (10–100 Å). We found that overex-

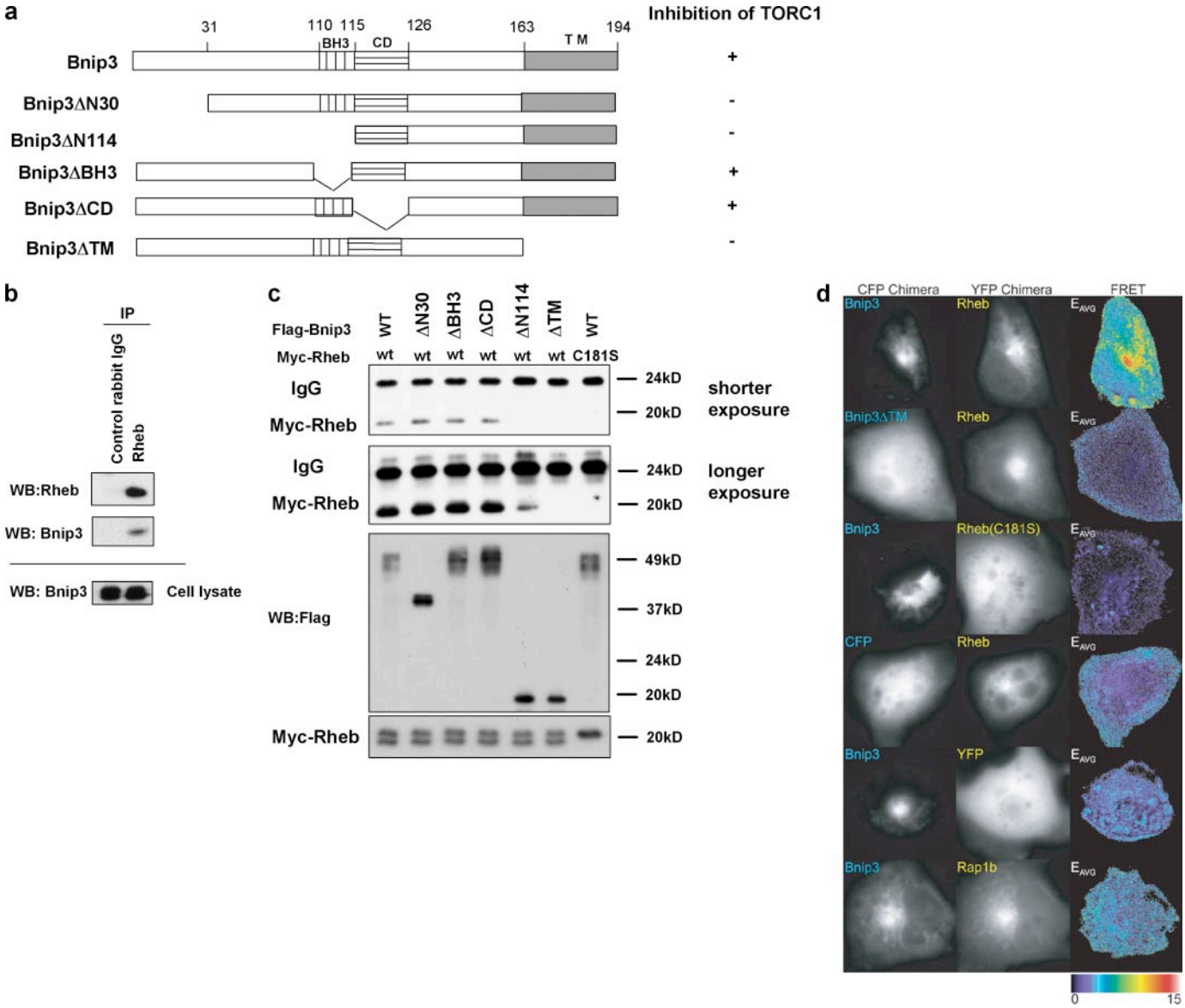

FIGURE 1. **Interaction between Rheb and Bnip3.** *a*, schematic domain structure of Bnip3. Domains are not drawn to scale. Inhibition of TORC1 as indicated was measured by immunoblotting for phosphorylation of S6K. *b*, co-immunoprecipitation of endogenous proteins. Cell lysate was prepared from mouse liver and treated with cross-linking reagent dithiobis(succinimidyl propionate). IP was performed with anti-Rheb or control rabbit IgG. The immunoprecipitated samples were detected by Western blotting (*WB*) with either Rheb or Bnip3 antibody as indicated. The expression levels of Bnip3 in the liver cell lysate are shown in the *bottom panel*. *c*, the N-terminal domain and transmembrane domain of Bnip3 are important for interaction with Rheb. Various FLAG-tagged Bnip3 deletion constructs were co-transfected with Myc-tagged Rheb in HEK293 cells. Cell lysate was immunoprecipitated with anti-FLAG antibody. Co-immunoprecipitation of Myc-Rheb was detected by anti-Myc Western blot (two exposures are shown in the *top two panels*). The immunoprecipitated Bnip3 proteins are detected by Western blot with anti-FLAG (*second panel* from the *bottom*). The expression levels of Myc-Rheb in cell lysate are shown in the *bottom panel*. *d*, interaction between Bnip3 and Rheb was determined by FRET. CFP-Bnip3 fusion plasmid was co-transfected in YFP-Rheb as indicated. Bnip3ΔTM and Rheb(C181S) mutant were included as indicated. Control of CFP, YFP, and Rap1b were included as negative controls. The *first and second columns* show fluorescence signal of CFP and YFP, respectively. The *last column* shows signal of FRET. The *scale* for fluorescence is indicated at the *bottom right*.

pression of YFP-Bnip3 or CFP-Rheb showed granule-like fluorescence pattern in cytoplasm (Fig. 1*d*). In contrast, Bnip3ΔTM and Rheb(C181S) mutants showed homogenous cytoplasmic distribution. These observations demonstrate that the TM domain in Bnip3 and the Cys^{181} in Rheb are important for subcellular localization of these two proteins. Supporting the co-IP results in HEK293 cells, Bnip3 showed strong interaction with Rheb as determined by the FRET (Fig. 1*d*). In contrast, no FRET was observed between Bnip3ΔTM and Rheb; nor was it observed between Bnip3 and Rheb(C181S). Bnip3ΔN30, Bnip3ΔCD, and Bnip3ΔBH3 also displayed a FRET-positive interaction with Rheb (data not shown). As expected, Bnip3 does not interact with Rap1b, although the two proteins show similar subcellular distribution (Fig. 1*d*). These results further support the interaction between Rheb and Bnip3.

Bnip3 Inhibits Phosphorylation of S6K Thr^{389}—Rheb stimulates S6K phosphorylation and activation via mTOR. Phosphorylation of S6K is a convenient and reliable measurement for mTOR activity *in vivo*. Therefore, we examined whether Bnip3 modulates the function of Rheb by measuring S6K phosphoryl-

ation. In HEK293 cells, overexpression of FLAG-Bnip3 inhibited the phosphorylation of the co-transfected HA-S6K1 in a dose-dependent manner (Fig. 2*a*). Surprisingly, the Bnip3L, which shares more than 50% sequence identity with Bnip3 and can also bind Rheb, did not have any effect on S6K phosphorylation. These observations strongly suggest that the inhibitory effect of Bnip3 depends on a specific sequence unique in Bnip3 and that mere binding to Rheb is not sufficient to inhibit the ability of Rheb in mTOR activation. 4EBP1 is another target of mTOR. mTOR phosphorylates 4EBP1 at multiple sites, including serine 65. To confirm the inhibitory effect of Bnip3 on mTOR signaling, we examined the effect of Bnip3 on 4EBP1 phosphorylation. Our results showed that Bnip3 but not Bnip3L inhibited 4EBP1 phosphorylation (Fig. 2*b*). These observations are consistent with a model in which Bnip3 inhibits mTOR activation by Rheb.

Since the Bnip3L has no effect on S6K and 4EBP1 phosphorylation, we focused on Bnip3 in subsequent studies. To further confirm weather Bnip3 inhibits S6K by acting through mTOR, we tested the rapamycin-resistant mutant, S6K-ΔC104, which contains a C-terminal deletion, and its phosphorylation of Thr^{389} is no longer inhibited by rapamycin (61). We found that Bnip3 could not inhibit phosphorylation of S6K-ΔC104 (Fig. 2*c*). These results suggest that the inhibitory effect of Bnip3 on S6K probably goes through mTOR. Recently, it has been established that the mTOR exists in two functionally distinct complexes, TORC1 and TORC2 (3). TORC1 is responsible for S6K Thr^{389} phosphorylation, whereas TORC2 phosphorylates AKT Ser^{473}. To check whether Bnip3 inhibits TORC2 activity, we examined the effect of Bnip3 overexpression on phosphorylation of GST-Akt. Our results demonstrate that Bnip3 is unable to inhibit the phosphorylation of Akt. This finding implies that Bnip3 specifically inhibits TOCR1 functions but not TOCR2 (Fig. 2*d*). Our data are consistent with the notion that Rheb is not directly involved in TORC2 activation (32).

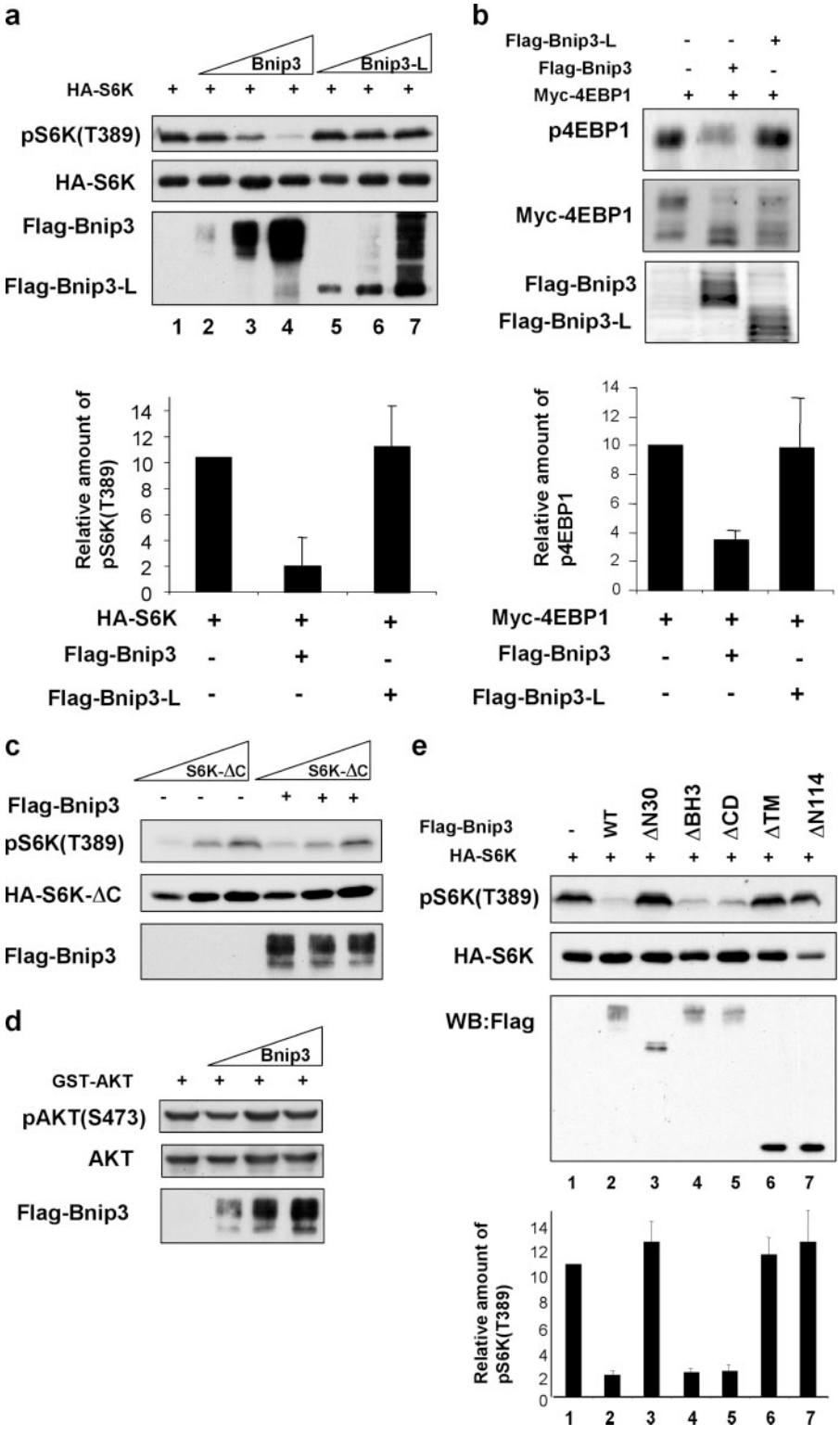

To map the sequence in Bnip3 required for S6K inhibition, several Bnip3 mutants were co-transfected with HA-S6K (Fig. 2*e*). Bnip3 wild type could potently inhibit S6K phosphorylation. Deletion of BH3 domain and CD had no effect on the ability of Bnip3 to inhibit S6K. As anticipated, Bnip3ΔTM completely lost its ability to inhibit S6K, because this mutant could not bind Rheb (Fig. 1, *c* and *d*). Bnip3ΔN30, which could bind

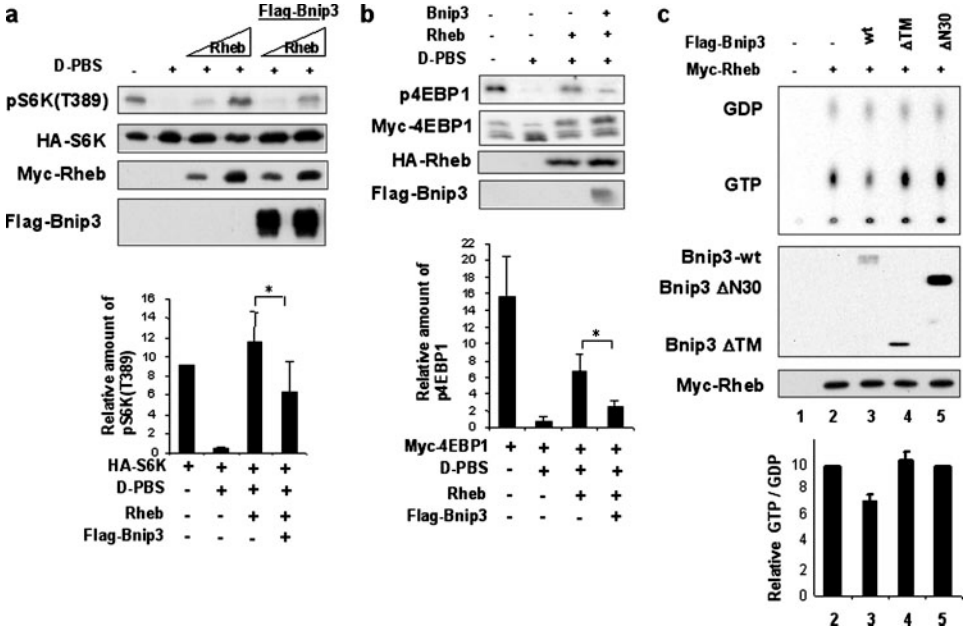

FIGURE 3. **Inhibition of Rheb function by Bnip3.** *a*, Bnip3 inhibits the Rheb-induced S6K phosphorylation. HA-S6K was co-transfected with Myc-Rheb and/or FLAG-Bnip3 as indicated. The transfected cells were incubated in Dulbecco's phosphate-buffered saline for 0.5 h as indicated. Phosphorylation of S6K was determined. The *bar graph* at the *bottom* shows quantification of S6K phosphorylation. Bnip3 significantly inhibited Rheb-induced S6K phosphorylation (*, $p < 0.01$). *b*, Bnip3 inhibits the Rheb-induced 4EBP1 phosphorylation. Experiments were similar to those in *A*. Phosphorylation of the co-transfected 4EBP1 was determined by Western blotting with anti-phospho(Ser^{65})-4EBP1 antibody. The *bar graph* at the *bottom* shows quantification of 4EBP1 phosphorylation. Bnip3 significantly inhibited Rheb-induced 4EBP1 phosphorylation (*, $p < 0.01$). *c*, Bnip3 inhibits Rheb GTP level. Myc-Rheb was transfected into HEK293 cells in the presence or absence of FLAG-Bnip3. The transfected cells were labeled with [^{32}P]phosphate, and Myc-Rheb was immunoprecipitated. The amounts of GTP and GDP bound to the precipitated Myc-Rheb were determined by thin layer chromatography (*top*). The Myc-Rheb in the immunoprecipitation and the expression levels of Bnip3 were detected by Western blot. Representative results of autoradiography and Western blot of three independent experiments are shown. The *bar graph* at the *bottom* shows quantification of the GTP/GDP ratio in immunoprecipitated Rheb.

Rheb at a similar level as the wild type Bnip3, however, also lost its activity completely (Fig. 2*e*). As predicted, Bnip3-ΔN114 could not inhibit S6K phosphorylation. These results suggest that interaction between Bnip3 and Rheb is necessary but not sufficient to inhibit Rheb function. Furthermore, our data indicate that the N-terminal region of Bnip3 is required to inhibit the mTOR pathway. Interestingly, the N-terminal region is not conserved between Bnip3 and Bnip3L, consistent with the observation that Bnip3L cannot inhibit mTOR, although it binds Rheb (Fig. 2*a*). Given the fact that Bnip3 and Bnip3L have no homology in their N-terminal 30 amino acids but share 65% identity in the rest of the protein, the above results strongly suggested that the N-terminal 30 amino acids of Bnip3 are essential for S6K inhibition.

Bnip3 Inhibits the Ability of Rheb to Induce S6K Phosphorylation—To examine whether Bnip3 affects the Rheb-induced S6K phosphorylation, Bnip3 was co-transfected with Myc-Rheb into HEK293 cells. Cells were treated with Dulbecco's phosphate-buffered saline to reduce the basal S6K phosphorylation; therefore, the Dulbecco's phosphate-buffered saline treatment highlighted the stimulatory effect of Rheb on S6K. Overexpression of FLAG-Bnip3 compromised the S6K phosphorylation induced by Rheb co-expression (Fig. 3*a*). We also examined the phosphorylation of 4EBP1, another substrate of TORC1. FLAG-Bnip3 inhibited the Rheb-induced 4EBP1 phosphorylation (Fig. 3*b*). The data in Fig. 2 indicate that mere binding is not sufficient for Bnip3 to inhibit Rheb function.

To investigate how Bnip3 affects Rheb function, we tested the Rheb GTP/GDP ratio by overexpressing Bnip3 and Rheb in HEK293 cells. Overexpression of wild type Bnip3 reproducibly decreased the GTP/GDP ratio by ~30% (Fig. 3*c*). Although the effect of Bnip3 on the Rheb GTP/GDP ratio is moderate, this change in Rheb GTP/GDP is rather significant. In similar experiments, we could not detect a change in Rheb GTP/GDP under various conditions, including insulin stimulation and amino acid addition.[3] Further supporting the importance of Bnip3 to Rheb GTP levels, we tested Bnip3ΔTM and Bnip3ΔN30, which lost the ability to inhibit S6K phosphorylation (Fig. 2*e*). We found that neither Bnip3ΔTM nor Bnip3ΔN30 affected Rheb GTP levels

[3] Y. Li, Y. Wang, E. Kim, P. Beemiller, C.-Y. Wang, J. Swanson, M. You, and K.-L. Guan, unpublished data.

FIGURE 2. **Inhibition of S6K phosphorylation by Bnip3.** *a*, Bnip3 but not Bnip3L inhibits S6K phosphorylation. HA-S6K was co-transfected with increasing amount of Bnip3 or Bnip3L into HEK293 cells as indicated. Phosphorylation of the co-transfected S6K was determined by Western blotting with anti-phospho-S6K antibody. The protein level of HA-S6K was determined by anti-HA. Western blot with anti-FLAG antibody was performed to detect the expression levels of FLAG-Bnip3 and Bnip3L (*bottom*). The *bar graph* at the *bottom* shows quantification of S6K phosphorylation ($n = 3$). The data represent S6K phosphorylation in *lanes 1*, *4*, and *7*, which have the highest levels of Bnip3 or Bnip3L. *Bars*, means ± S.E. for relative S6K phosphorylation levels. Bnip3 significantly inhibits S6K phosphorylation ($p < 0.01$). *b*, Bnip3 but not Bnip3L inhibits 4EBP1 phosphorylation. Experiments were similar to those in *a*. Phosphorylation of the co-transfected 4EBP1 was determined by Western blotting with anti-phospho(Ser^{65})-4EBP1 antibody. The *bar graph* at the *bottom* shows quantification of 4EBP1 phosphorylation ($n = 3$). Bnip3 significantly inhibits 4EBP1 phosphorylation ($p < 0.01$). *c*, Bnip3 does not inhibit the phosphorylation of the rapamycin-insensitive S6K-ΔC. HA-S6K-ΔC contains a deletion in its C-terminal region. Phosphorylation of this mutant S6K is not inhibited by rapamycin; therefore, S6K-ΔC is not phosphorylated by TORC1. HA-S6K-ΔC was transfected into HEK293 cells in the presence or absence of Bnip3 as indicated. Phosphorylation of S6K-ΔC was determined by Western blotting with anti-phospho-S6K antibody. *d*, Bnip3 does not inhibit Akt phosphorylation. GST-Akt was transfected with increasing amounts of Bnip3. Phosphorylation of Akt-Ser^{473}, which is the TORC2 phosphorylation site, was determined by anti-phospho-Ser^{473}-specific antibody. *e*, the N-terminal domain and transmembrane domain of Bnip3 are required for S6K inhibition. HA-S6K was co-transfected with various FLAG-tagged Bnip3 mutants. Phosphorylation of the co-transfected HA-S6K was determined. The expression levels of Bnip3 constructs were determined by Western with anti-FLAG antibody. The *bar graph* at the *bottom* shows quantification of S6K inhibition by various Bnip3 mutants ($n = 3$).

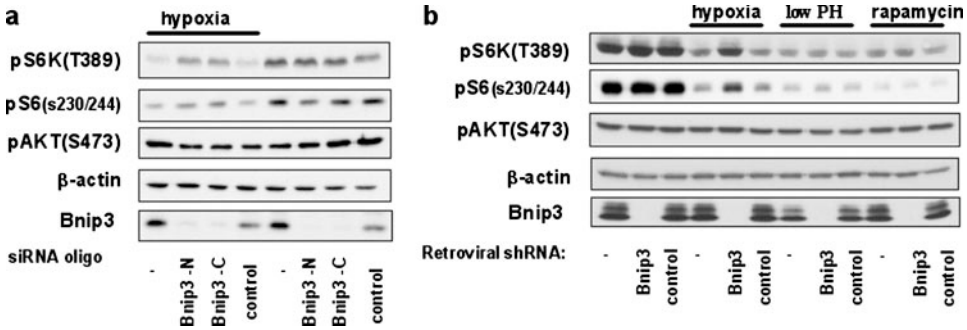

FIGURE 4. **Involvement of Bnip3 in hypoxia-induced mTOR inhibition.** *a*, Bnip3 knockdown relieves the inhibition on mTOR by hypoxia. Two Bnip3 siRNAs targeting for the N-terminal (Bnip3-N) and C-terminal (Bnip3-C) region were independently transfected into HEK293 cells. Transfection of control siRNA is also indicated. Phosphorylation of endogenous S6K, S6, and AKT were determined by phosphospecific antibodies. The protein levels of endogenous Bnip3 were also determined. Hypoxia treatment is indicated. *b*, Bnip3 specifically suppresses the hypoxia effect on S6K phosphorylation. Retroviral shRNA targeting for Bnip3 or control was used to infect HEK293 cells. The virus-infected cells were selected by resistance to puromycin. Cells were exposed to hypoxia (1 h), low pH cultural medium (12 h), or rapamycin (1 nM, 30 min) as indicated. Phosphorylation of endogenous S6K and AKT were determined by Western blot with phosphospecific antibodies as indicated. Knockdown of Bnip3 in the stable cell line was confirmed by Western blot with anti-Bnip3 antibody (*bottom*).

(Fig. 3*c*). Besides TSC2, Bnip3 is the only protein known to affect Rheb GTP/GDP in our studies. Therefore, our data indicate that Bnip3 inhibits the mTOR pathway by decreasing Rheb GTP levels.

Bnip3 Is Required for Hypoxia-induced S6K Inhibition—We used siRNA oligonucleotides to test the effect of endogenous Bnip3 on S6K phosphorylation and S6K kinase activity, which was measured by checking the phosphorylation of S6, a direct substrate of S6K. Two RNA duplexes, corresponding to either an amino-terminal (Bnip3-N) or C-terminal (Bnip3-C) region of Bnip3, were used to suppress expression of endogenous Bnip3. Transfection of siRNA-C or siRNA-N caused a significant reduction of endogenous Bnip3 protein levels in HEK293 cells, whereas Bnip3 siRNA had no effect on expression levels of the β-actin control (Fig. 4*a*). It is worth noting that in contrast to a strong induction of Bnip3 by hypoxia in many cell lines, Bnip3 is expressed in HEK293 cells, and its expression is not significantly induced by 1 h of exposure to hypoxia. We found that Bnip3 knockdown had little effect on the basal phosphorylation of S6K and S6. Hypoxia inhibited S6K phosphorylation. Interestingly, Bnip3 knockdown significantly blocked the inhibition of S6K phosphorylation in response to hypoxia (Fig. 4*a*). Control experiments with unrelated siRNA oligonucleotides had no effect on the phosphorylation of S6K and S6. This observation suggests that Bnip3 may be specifically activated under hypoxia and plays a critical role in mTOR inhibition in response to hypoxia.

To further confirm the specific function of Bnip3 in hypoxia response, we established a Bnip3 knockdown stable cell line. HEK293 cells were infected by retrovirus expressing Bnip3 shRNA and control shRNA, respectively. The stable shRNA expressing cells were selected by puromycin. Bnip3 protein was greatly reduced in the Bnip3-shRNA-expressing cell lines (Fig. 4*b*). Consistent with the transient siRNA transfection results in Fig. 4*a*, stable Bnip3 knockdown blocked the decrease of phosphorylation of S6K and S6 in response to hypoxia conditions but had no effect on phosphorylation of Akt (Fig. 4*b*). We also examined if the effect of Bnip3 is specific to hypoxia response. Both hypoxia and low pH (pH 6.5) caused a similar reduction in phosphorylation of S6K and S6. Bnip3 knockdown only suppressed the effect of hypoxia and not the effect of low pH (Fig. 4*b*). These results suggest that Bnip3 is specifically involved in hypoxia response. In addition, cells were treated with a low dose of rapamycin to partially inhibit TORC1 activity to a degree similar to those inhibited by either hypoxia or low pH. Bnip3 siRNA could not block the inhibitory effect of rapamycin on S6K (Fig. 4*b*). These data suggest that Bnip3 acts specifically in hypoxia response upstream of TORC1. Moreover, the above results are consistent with our observations that Bnip3 binds to Rheb and decreases Rheb GTP levels.

Bnip3 Knockdown Provides an mTOR-dependent Growth Advantage in Vivo—Bnip3 has been implicated in tumor development. A possible mechanism of Bnip3 in cancer inhibition is due to its activity in promoting cell death. It is also possible that Bnip3 may inhibit tumor growth by inhibiting mTOR, especially in solid tumors, which are frequently under hypoxia conditions. We tested the effect of Bnip3 knockdown on tumor formation in nude mice. Both Bnip3 knockdown and control HEK293 cells were injected into nude mice. Tumor size was monitored. We found that the Bnip3 knockdown cells formed much bigger tumors than the control cells (Fig. 5, *a–c*). These data indicate that the elevated mTOR activity in the Bnip3 knockdown cells may provide a growth advantage. To further test the function of mTOR activation in Bnip3-induced tumor growth, we treated the mice with rapamycin, which should inhibit mTOR even in Bnip3 knockdown cells. As expected, rapamycin significantly inhibited tumor growth of HEK293 cells (Fig. 5, *d–f*). Interestingly, the Bnip3 knockdown cells did not show any growth advantage over the control cells in the presence of rapamycin. These results strongly indicate that the elevated mTOR activity by Bnip3 knockdown is responsible for the growth advantage of the Bnip3 knockdown in HEK293 cells *in vivo*.

DISCUSSION

TOR is a central controller of cell growth and cell size and is regulated by a variety of extracellular stimuli, including growth factor, nutrient deprivation, and stress (3, 62). It is well established that the mTOR pathway is inhibited by hypoxia (38, 63). The molecular mechanism of mTOR inactivation by hypoxia is not fully understood. We showed in this report that Bnip3 can directly bind to Rheb and inhibits TORC1. Our data indicate that Bnip3 plays a direct role in mediating the TORC1 inhibition in response to hypoxia. We also showed that Bnip3 inhibits TORC1 but not TORC2.

Several lines of evidence are presented in this report to support a role of Bnip3 in TORC1 regulation. First, Bnip3 inhibits

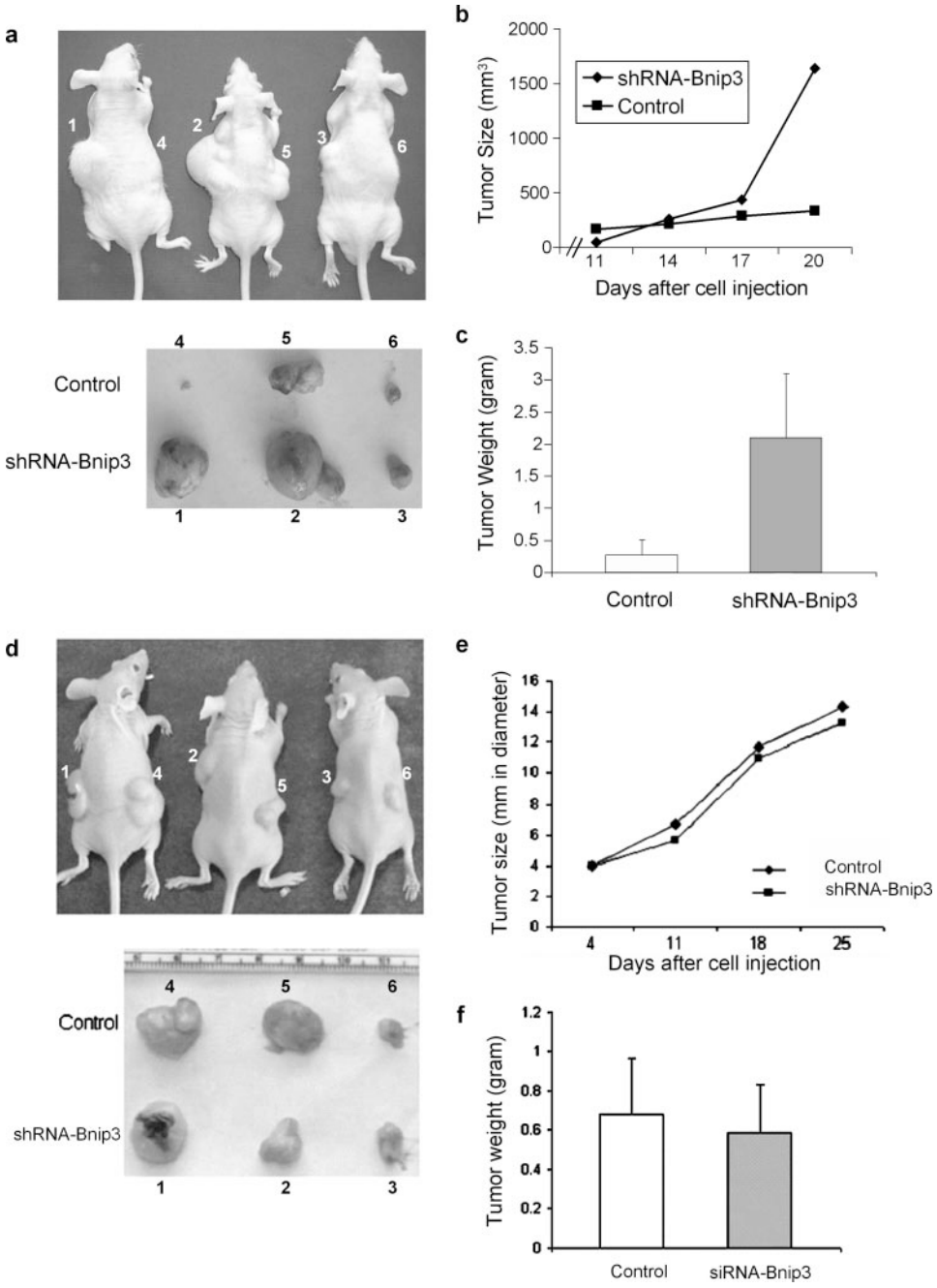

FIGURE 5. **Rapamycin suppresses growth advantage of Bnip3 knockdown cells in nude mice.** *a–c*, Bnip3 knockdown HEK293 cells grow faster in nude mice. Pictures of tumor growth of three representative mice are shown in *a*. Equal amounts of HEK293 cells stably infected with shRNA for Bnip3 or control were injected into the left or right side of each mouse, respectively. Each tumor was labeled with a specific number. Tumor growth of control or Bnip3 knockdown cells was monitored (*b* and *c*). *d–f*, rapamycin suppresses the growth advantage of Bnip3 knockdown cells. Experiments were similar to those in *a–c*, except the mice were treated with rapamycin. In the presence of rapamycin, the Bnip3 knockdown cells grew at a rate similar to the control cells. The *scale* in *f* is different from that in *c*.

the phosphorylation of S6K and S6 but has little effect on AKT phosphorylation. Bnip3 also inhibits phosphorylation of another TORC1 substrate 4EBP1. Second, Bnip3 directly binds to Rheb. The interaction between Bnip3 and Rheb are confirmed by experiments of yeast two-hybrid assay, co-immunoprecipitation, and FRET. Third, Bnip3 decreases Rheb GTP level, thus providing a possible biochemical mechanism of how Bnip3 inhibits Rheb. Fourth, down-regulation of Bnip3 significantly suppresses the TORC1 inhibition in response to hypoxia. This finding suggests that Bnip3 plays an important role in TORC1 regulation. Finally, the Bnip3 knockdown cells grow faster than the control cells in nude mice, indicating a growth advantage of Bnip3 knockdown cells. Moreover, rapamycin effectively inhibits the growth advantage of Bnip3 knockdown cells *in vivo*. Therefore, the growth advantage caused by Bnip3 knockdown is mainly due to activation of TORC1. Our data establish an important role of Bnip3 in hypoxia response in regulation of cell growth by binding Rheb and inhibiting the TORC1 pathway.

Both long term and short term hypoxia can inhibit mTOR. It has been shown that the short term inhibition of the mTOR signaling pathway by hypoxia is hypoxia-inducible factor (HIF) (a transcription factor)-independent (63). Consistently, we observed that 1-h hypoxia treatment efficiently inhibited TORC1 signaling in HEK293 cells, whereas Bnip3 protein level was not significantly increased within the short hypoxia treatment. Interestingly, hypoxia failed to inhibit TORC1 function in Bnip3 knockdown cells. Our results suggest that Bnip3 mediates the rapid inhibitory effect of hypoxia on TORC1. In contrast, knockdown of Bnip3 has no effect on TORC1 signaling in response to other stress conditions, indicating that the effect of Bnip3 on TORC1 is specific to hypoxia response. It is possible that hypoxia may increase Bnip3 activity by an unknown mechanism. It is also possible the Bnip3 may collaborate with another signaling component that is rapidly activated by hypoxia to inhibit TORC1.

Bnip3 expression is induced by hypoxia in many different cell types (41). The induction is mainly at the level of transcription and is mediated via HIF-1 (64). We also observed that hypoxia induces BNIP3 mRNA expression at the 6-h time point. Therefore, it is likely that the HIF-mediated Bnip3 induction may play a role in TORC1 regulation in response to prolonged hypoxia. It is worth noting that two stress-inducible genes, Redd1 and Redd2, have been reported to inhibit the mTOR pathway (37–39). Both Redd1

and Redd2 appear to function upstream of TSC2, whereas the biochemical mechanism of Redd1 and Redd2 in TORC1 inhibition is unknown. In contrast, our data show that Bnip3 acts directly on Rheb, which is the direct downstream target of TSC2 and upstream activator of TORC1. Therefore, hypoxia may suppress TORC1 activity by multiple mechanisms, including the induction of Bnip3 and Redd. However, Bnip3 and Redd inhibit TORC1 by acting at different levels in the pathway, one at Rheb and the other upstream of TSC1/2, respectively.

Most solid tumors are constantly exposed to hypoxia. The ability of tumor cells to grow and survive under hypoxia condition is extremely important for tumor development. Interestingly, silence of Bnip3 expression has been reported in some tumors (50, 65–67). Based on our observations, we propose a model of how hypoxia inhibits the mTOR pathway and cell growth. Hypoxia induces the expression and activation of the Bnip3, which then binds to and inhibits Rheb. The precise molecular mechanisms how Bnip3 inhibits Rheb remain to be elucidated. However, our results show that inhibition of Rheb by Bnip3 requires at least two activities; one is binding, and the other is decreasing Rheb GTP levels. Bnip3 may inhibit Rheb function by preventing its interaction with downstream effectors. It may also inhibit Rheb function by interfering with the nucleotide exchange of Rheb, such as interfering with the interaction with Rheb guanine nucleotide exchange factor. Future studies are needed to address these important questions in Rheb signaling. In summary, our study has identified Bnip3 as a critical component in TORC1 regulation by hypoxia. Our observations may explain why some tumor cells have reduced Bnip3 expressions. A reduction of Bnip3 may be advantageous to tumor cells by increasing growth due to a high mTOR activity and decreasing apoptosis, especially under hypoxia conditions.

Acknowledgment—We thank Dr. Ken Inoki for discussions.

REFERENCES

1. Hay, N., and Sonenberg, N. (2004) *Genes Dev.* **18,** 1926–1945
2. Inoki, K., Ouyang, H., Li, Y., and Guan, K. L. (2005) *Microbiol. Mol. Biol. Rev.* **69,** 79–100
3. Wullschleger, S., Loewith, R., and Hall, M. N. (2006) *Cell* **124,** 471–484
4. Inoki, K., and Guan, K. L. (2006) *Trends Cell Biol.* **16,** 206–212
5. Jacinto, E., Facchinetti, V., Liu, D., Soto, N., Wei, S., Jung, S. Y., Huang, Q., Qin, J., and Su, B. (2006) *Cell* **127,** 125–137
6. Jacinto, E., Loewith, R., Schmidt, A., Lin, S., Ruegg, M. A., Hall, A., and Hall, M. N. (2004) *Nat. Cell Biol.* **6,** 1122–1128
7. Frias, M. A., Thoreen, C. C., Jaffe, J. D., Schroder, W., Sculley, T., Carr, S. A., and Sabatini, D. M. (2006) *Curr. Biol.* **16,** 1865–1870
8. Loewith, R., Jacinto, E., Wullschleger, S., Lorberg, A., Crespo, J. L., Bonenfant, D., Oppliger, W., Jenoe, P., and Hall, M. N. (2002) *Mol. Cell* **10,** 457–468
9. Sarbassov, D. D., Ali, S. M., Kim, D. H., Guertin, D. A., Latek, R. R., Erdjument-Bromage, H., Tempst, P., and Sabatini, D. M. (2004) *Curr. Biol.* **14,** 1296–1302
10. Yang, Q., Inoki, K., Ikenoue, T., and Guan, K. L. (2006) *Genes Dev.* **20,** 2820–2832
11. Sancak, Y., Thoreen, C. C., Peterson, T. R., Lindquist, R. A., Kang, S. A., Spooner, E., Carr, S. A., and Sabatini, D. M. (2007) *Mol. Cell* **25,** 903–915
12. Vander Haar, E., Lee, S. I., Bandhakavi, S., Griffin, T. J., and Kim, D. H. (2007) *Nat. Cell Biol.* **9,** 316–323
13. Sarbassov, D. D., Guertin, D. A., Ali, S. M., and Sabatini, D. M. (2005) *Science* **307,** 1098–1101
14. Kwiatkowski, D. J. (2003) *Ann. Hum. Genet.* **67,** 87–96
15. Garami, A., Zwartkruis, F. J., Nobukuni, T., Joaquin, M., Roccio, M., Stocker, H., Kozma, S. C., Hafen, E., Bos, J. L., and Thomas, G. (2003) *Mol. Cell* **11,** 1457–1466
16. Inoki, K., Li, Y., Xu, T., and Guan, K. L. (2003) *Genes Dev.* **17,** 1829–1834
17. Castro, A. F., Rebhun, J. F., Clark, G. J., and Quilliam, L. A. (2003) *J. Biol. Chem.* **278,** 32493–32496
18. Saucedo, L. J., Gao, X., Chiarelli, D. A., Li, L., Pan, D., and Edgar, B. A. (2003) *Nat. Cell Biol.* **5,** 566–571
19. Stocker, H., Radimerski, T., Schindelholz, B., Wittwer, F., Belawat, P., Daram, P., Breuer, S., Thomas, G., and Hafen, E. (2003) *Nat. Cell Biol.* **5,** 559–565
20. Tee, A. R., Manning, B. D., Roux, P. P., Cantley, L. C., and Blenis, J. (2003) *Curr. Biol.* **13,** 1259–1268
21. Zhang, Y., Gao, X., Saucedo, L. J., Ru, B., Edgar, B. A., and Pan, D. (2003) *Nat. Cell Biol.* **5,** 578–581
22. Urano, J., Comiso, M. J., Guo, L., Aspuria, P. J., Deniskin, R., Tabancay, A. P., Jr., Kato-Stankiewicz, J., and Tamanoi, F. (2005) *Mol. Microbiol.* **58,** 1074–1086
23. Long, X., Lin, Y., Ortiz-Vega, S., Yonezawa, K., and Avruch, J. (2005) *Curr. Biol.* **15,** 702–713
24. Dan, H. C., Sun, M., Yang, L., Feldman, R. I., Sui, X. M., Ou, C. C., Nellist, M., Yeung, R. S., Halley, D. J., Nicosia, S. V., Pledger, W. J., and Cheng, J. Q. (2002) *J. Biol. Chem.* **277,** 35364–35370
25. Goncharova, E. A., Goncharov, D. A., Eszterhas, A., Hunter, D. S., Glassberg, M. K., Yeung, R. S., Walker, C. L., Noonan, D., Kwiatkowski, D. J., Chou, M. M., Panettieri, R. A., Jr., and Krymskaya, V. P. (2002) *J. Biol. Chem.* **277,** 30958–30967
26. Manning, B. D., Tee, A. R., Logsdon, M. N., Blenis, J., and Cantley, L. C. (2002) *Mol. Cell* **10,** 151–162
27. Inoki, K., Li, Y., Zhu, T., Wu, J., and Guan, K. L. (2002) *Nat. Cell Biol.* **4,** 648–657
28. Inoki, K., Ouyang, H., Zhu, T., Lindvall, C., Wang, Y., Zhang, X., Yang, Q., Bennett, C., Harada, Y., Stankunas, K., Wang, C. Y., He, X., MacDougald, O. A., You, M., Williams, B. O., and Guan, K. L. (2006) *Cell* **126,** 955–968
29. Inoki, K., Zhu, T., and Guan, K. L. (2003) *Cell* **115,** 577–590
30. Aspuria, P. J., and Tamanoi, F. (2004) *Cell. Signal.* **16,** 1105–1112
31. Manning, B. D., and Cantley, L. C. (2003) *Trends Biochem. Sci.* **28,** 573–576
32. Yang, Q., Inoki, K., Kim, E., and Guan, K. L. (2006) *Proc. Natl. Acad. Sci. U. S. A.* **103,** 6811–6816
33. Li, Y., Inoki, K., and Guan, K. L. (2004) *Mol. Cell. Biol.* **24,** 7965–7975
34. Long, X., Ortiz-Vega, S., Lin, Y., and Avruch, J. (2005) *J. Biol. Chem.* **280,** 23433–23436
35. Nobukuni, T., Joaquin, M., Roccio, M., Dann, S. G., Kim, S. Y., Gulati, P., Byfield, M. P., Backer, J. M., Natt, F., Bos, J. L., Zwartkruis, F. J., and Thomas, G. (2005) *Proc. Natl. Acad. Sci. U. S. A.* **102,** 14238–14243
36. Roccio, M., Bos, J. L., and Zwartkruis, F. J. (2006) *Oncogene* **25,** 657–664
37. Reiling, J. H., and Hafen, E. (2004) *Genes Dev.* **18,** 2879–2892
38. Brugarolas, J., Lei, K., Hurley, R. L., Manning, B. D., Reiling, J. H., Hafen, E., Witters, L. A., Ellisen, L. W., and Kaelin, W. G., Jr. (2004) *Genes Dev.* **18,** 2893–2904
39. Corradetti, M. N., Inoki, K., and Guan, K. L. (2005) *J. Biol. Chem.* **280,** 9769–9772
40. Boyd, J. M., Malstrom, S., Subramanian, T., Venkatesh, L. K., Schaeper, U., Elangovan, B., D'Sa-Eipper, C., and Chinnadurai, G. (1994) *Cell* **79,** 341–351
41. Lee, H., and Paik, S. G. (2006) *Mol. Cells* **21,** 1–6
42. Yasuda, M., D'Sa-Eipper, C., Gong, X. L., and Chinnadurai, G. (1998) *Oncogene* **17,** 2525–2530
43. Chen, G., Ray, R., Dubik, D., Shi, L., Cizeau, J., Bleackley, R. C., Saxena, S., Gietz, R. D., and Greenberg, A. H. (1997) *J. Exp. Med.* **186,** 1975–1983
44. Ray, R., Chen, G., Vande Velde, C., Cizeau, J., Park, J. H., Reed, J. C., Gietz, R. D., and Greenberg, A. H. (2000) *J. Biol. Chem.* **275,** 1439–1448
45. Vande Velde, C., Cizeau, J., Dubik, D., Alimonti, J., Brown, T., Israels, S., Hakem, R., and Greenberg, A. H. (2000) *Mol. Cell. Biol.* **20,** 5454–5468
46. Daido, S., Kanzawa, T., Yamamoto, A., Takeuchi, H., Kondo, Y., and

Kondo, S. (2004) *Cancer Res.* **64,** 4286–4293
47. Guo, K., Searfoss, G., Krolikowski, D., Pagnoni, M., Franks, C., Clark, K., Yu, K. T., Jaye, M., and Ivashchenko, Y. (2001) *Cell Death Differ.* **8,** 367–376
48. Bruick, R. K. (2000) *Proc. Natl. Acad. Sci. U. S. A.* **97,** 9082–9087
49. Webster, K. A., Graham, R. M., and Bishopric, N. H. (2005) *J. Mol. Cell Cardiol.* **38,** 35–45
50. Erkan, M., Kleeff, J., Esposito, I., Giese, T., Ketterer, K., Buchler, M. W., Giese, N. A., and Friess, H. (2005) *Oncogene* **24,** 4421–4432
51. Okami, J., Simeone, D. M., and Logsdon, C. D. (2004) *Cancer Res.* **64,** 5338–5346
52. Abe, T., Toyota, M., Suzuki, H., Murai, M., Akino, K., Ueno, M., Nojima, M., Yawata, A., Miyakawa, H., Suga, T., Ito, H., Endo, T., Tokino, T., Hinoda, Y., and Imai, K. (2005) *J. Gastroenterol.* **40,** 504–510
53. Manka, D., Spicer, Z., and Millhorn, D. E. (2005) *Cancer Res.* **65,** 11689–11693
54. Figueroa, C., Taylor, J., and Vojtek, A. B. (2001) *J. Biol. Chem.* **276,** 28219–28225
55. Matsushima, M., Fujiwara, T., Takahashi, E., Minaguchi, T., Eguchi, Y., Tsujimoto, Y., Suzumori, K., and Nakamura, Y. (1998) *Genes Chromosomes Cancer* **21,** 230–235
56. Chen, G., Cizeau, J., Vande Velde, C., Park, J. H., Bozek, G., Bolton, J., Shi, L., Dubik, D., and Greenberg, A. (1999) *J. Biol. Chem.* **274,** 7–10
57. Kim, J. Y., Cho, J. J., Ha, J., and Park, J. H. (2002) *Arch. Biochem. Biophys.* **398,** 147–152
58. Sulistijo, E. S., Jaszewski, T. M., and MacKenzie, K. R. (2003) *J. Biol. Chem.* **278,** 51950–51956
59. Sulistijo, E. S., and Mackenzie, K. R. (2006) *J. Mol. Biol.* **364,** 974–990
60. Clark, G. J., Kinch, M. S., Rogers-Graham, K., Sebti, S. M., Hamilton, A. D., and Der, C. J. (1997) *J. Biol. Chem.* **272,** 10608–10615
61. Weng, Q. P., Andrabi, K., Kozlowski, M. T., Grove, J. R., and Avruch, J. (1995) *Mol. Cell. Biol.* **15,** 2333–2340
62. Sarbassov, D. D., Ali, S. M., and Sabatini, D. M. (2005) *Curr. Opin. Cell Biol.* **17,** 596–603
63. Arsham, A. M., Howell, J. J., and Simon, M. C. (2003) *J. Biol. Chem.* **278,** 29655–29660
64. Sowter, H. M., Ratcliffe, P. J., Watson, P., Greenberg, A. H., and Harris, A. L. (2001) *Cancer Res.* **61,** 6669–6673
65. Murai, M., Toyota, M., Suzuki, H., Satoh, A., Sasaki, Y., Akino, K., Ueno, M., Takahashi, F., Kusano, M., Mita, H., Yanagihara, K., Endo, T., Hinoda, Y., Tokino, T., and Imai, K. (2005) *Clin. Cancer Res.* **11,** 1021–1027
66. Giatromanolaki, A., Koukourakis, M. I., Sowter, H. M., Sivridis, E., Gibson, S., Gatter, K. C., and Harris, A. L. (2004) *Clin. Cancer Res.* **10,** 5566–5571
67. Murai, M., Toyota, M., Satoh, A., Suzuki, H., Akino, K., Mita, H., Sasaki, Y., Ishida, T., Shen, L., Garcia-Manero, G., Issa, J. P., Hinoda, Y., Tokino, T., and Imai, K. (2005) *Br. J. Cancer* **92,** 1165–1172
68. Kim, D. H., Sarbassov, D. D., Ali, S. M., King, J. E., Latek, R. R., Erdjument-Bromage, H., Tempst, P., and Sabatini, D. M. (2002) *Cell* **110,** 163–175
69. Beemiller, P., Hoppe, A. D., and Swanson, J. A. (2006) *PLoS Biol.* **4,** 987–999
70. Eshleman, J. S., Carlson, B. L., Mladek, A. C., Kastner, B. D., Shide, K. L., and Sarkaria, J. N. (2002) *Cancer Res.* **62,** 7291–7297
71. Hoppe, A., Christensen, K., and Swanson, J. A. (2002) *Biophys. J.* **83,** 3652–3664